

Subband-Based Active Noise Equalizer for Motorcycle Helmets

Tongwei Wang^{*}, Woon S. Gan^{*}, Sen M. Kuo[†] and Yong Kim Chong^{*}

^{*}DSP Lab, School of Electrical and Electronic Engineering, Nanyang Technological University, Singapore
E-mail: ewsgan@ntu.edu.sg

[†]Department of Electrical Engineering, Northern Illinois University, DeKalb, IL, USA
E-mail: kuo@ceet.niu.edu

Abstract— Analysis shows that most energy of the motorcycle noise is concentrated at low frequencies. Active noise control (ANC) helmets provide good attenuation for such low-frequency noise that is difficult to reduce by passive methods. In addition, it does not completely cancel the motorcycle noise since in some cases it is desired to extract important sound information. This paper proposes the subband-based active noise equalizer (SBANE) for motorcycle helmets, which has advantages of reducing computational load, faster convergence rate and more refined noise control over traditional ANE system. Furthermore, we can incorporate psychoacoustics noise equalizer by using subband technique to better match the human perception. Computer simulations show the feasibility of using the proposed method for SBANE-based helmets.

I. INTRODUCTION

Motorcycle is a convenient and cheap form of transportation and there is an increasing demand for motorcycles worldwide. Unfortunately, the motorcycle noise acts as a silent killer. It is found that motorcycle noise levels on an open road are approximately from 78 to 90 dBA at 30 mph (miles-per-hour) and can be up to 116 dBA at 120 mph. Continuous exposure to noise level of 95 dBA for more than 2.5 hours may result in various hearing impairments such as hearing loss, tinnitus, acoustic shock and even leads to accidents. In addition, the motorcycle noise not only distracts the attention of the rider, but also degrades the speech quality in wireless communication.

Figure 1 illustrates the frequency spectrum of motorcycle noise recorded at 40 mph, which can be considered as a typical example of motorcycle noise. It shows dominant motorcycle noise components are concentrated at low frequencies below 500 Hz. Therefore, helmets based on active noise control (ANC) have been proposed in [1].

Although ANC system is able to attenuate low-frequency motorcycle engine noise [1], there is still a need for psychoacoustic shaping of residual noise spectrum to better match human preference. This demand leads to an extension of the ANC concept to include broadband active noise equalization (ANE) [2], which offers a complete control the shape of residual noise spectrum. Also, it is desired to retain a low-level residual noise with specific spectral shape in some occasions. For example, the motorcycle rider needs audible information about the engine speed in order to control the

vehicle safely. This task can be realized by a time-domain broadband active noise equalizer introduced in [2]. By shaping the motorcycle noise spectrum, we can promote safe riding habit because unpleasant noise can remind the rider of speed limit.

Conventional approach in broadband ANE requires a lot of computational load due to long filter length and operating at high sampling frequency. Convergence rate of the adaptive algorithm also suffers due to the long filter length and higher eigenvalue spread (spectral dynamic range) of the input signal.

Subband adaptive filtering technique [3] has been successfully applied to improve the convergence rate of the adaptive filter and reduces the computational complexity of high-order adaptive filters. The processing of signals in subbands not only reduces the computational burden because adaptive filtering is performed at a lower decimation rate, but also results in faster convergence because the spectral dynamic range is greatly reduced in each subband. Hence, this paper presents a subband-based ANE for motorcycle helmets that possess these advantages.

The rest of this paper is organized as follows. In Section 2, the conventional broadband ANE is introduced. The proposed subband-based ANE for motorcycle helmets is presented in Section 3. The performance of the proposed system is evaluated using computer simulations and shown in Section 4. Section 5 concludes this paper.

II. BROADBAND ACTIVE NOISE EQUALIZER

As shown in Fig. 2, the broadband ANE achieves the noise shaping using the shaping filter $C(z)$, which is designed so that the residual noise $e(n)$ has a similar spectrum shape as $|C(z)|^2$.

In computer simulation, the primary noise $d(n)$ is obtained by transmitting the reference noise $x(n)$ from a noise source through the primary path $P(z)$ as

$$d(n) = p(n) * x(n), \quad (1)$$

where n is the time index, $p(n)$ is the impulse response of $P(z)$ and $*$ denotes linear convolution. The adaptive output $y(n)$ is calculated as

$$y(n) = \mathbf{w}^T(n)\mathbf{x}(n), \quad (2)$$

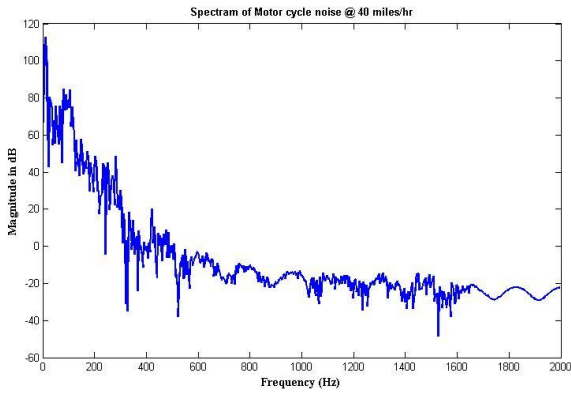


Fig. 1 Spectrum of motorcycle noise at 40 mph (adapted from [1])

where the M -tap adaptive weight vector is give by

$$\mathbf{w}(n) = [w_0(n) \quad w_1(n) \quad \cdots \quad w_{M-1}(n)]^T, \quad (3)$$

and the vector for the reference noise is give by

$$\mathbf{x}(n) = [x(n) \quad x(n-1) \quad \cdots \quad x(n-M+1)]^T. \quad (4)$$

The adaptive filter $W(z)$ minimizes the instantaneous pseudo-error $e'(n)$, instead of the residual noise $e(n)$ acquired by the error microphone. The weight-update equation utilizes the filtered-X least-mean-square (FXLMS) algorithm as

$$\mathbf{w}(n+1) = \mathbf{w}(n) + \mu \mathbf{x}'(n) e'(n), \quad (5)$$

where μ is step size for the FXLMS algorithm, and

$$\mathbf{x}'(n) = \hat{s}(n) * \mathbf{x}(n) \quad (6)$$

is the filtered version of $x(n)$, and $\hat{s}(n)$ is the impulse response of the estimated secondary path $\hat{S}(z)$. The pseudo-error $e'(n)$ is calculated as

$$e'(n) = e(n) - \hat{s}(n) * c(n) * y(n), \quad (7)$$

where $c(n)$ is the impulse response of the shaping filter $C(z)$. The cancelling noise $y'(n)$ is calculated as

$$y'(n) = -[y(n) - c(n) * y(n)]. \quad (8)$$

It propagates through the secondary path $S(z)$, resulting in $y''(n) = s(n) * y'(n)$, where $s(n)$ is the actual impulse response of the secondary path $S(z)$.

Assuming that $W(z)$ has sufficient order, and we have perfect estimation of the secondary path, i.e., $\hat{S}(z) = S(z)$, the residual noise in steady state can be expressed as

$$E(z) = P(z)X(z) - S(z)[1 - C(z)]Y(z). \quad (9)$$

Since $W(z)$ has been assumed to have sufficient order, it would converge to the optimal solution given as $W^o(z) = P(z)/S(z)$. Then the corresponding optimal residual error (in z -domain) would be given as

$$E^o(z) = C(z)P(z)X(z).$$

Therefore, the residual noise $e(n)$ is completely controlled by the shaping filter $C(z)$.

III. PROPOSED SUBBAND-BASED ACTIVE NOISE EQUALIZER FOR MOTORCYCLE HELMETS

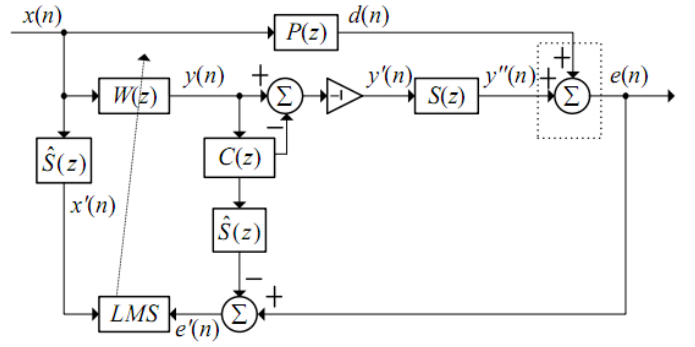


Fig. 2 Block diagram of conventional broadband ANE

The positions of the microphones and secondary sources for motorcycle helmets are shown in Fig. 4, and the block diagram of the proposed SBANE is shown in Fig. 3. Basically, the fullband motorcycle noise is decomposed into N spectral bands using analysis filters $H_i(z)$, $i = 0, 1, \dots, N-1$. These subband signals $x_i(n)$ are decimated to a lower rate by a factor of D . Subsequently, the decimated subband signals $x_{i,D}(n)$ are processed by individual subband adaptive filters $W_i(z)$. Each subband adaptive filter has its individual adaptation loop with their corresponding subband shaping filter $C_i(z)$ and secondary path estimate $\hat{S}_i(z)$. After obtaining those subband cancelling noises $y'_i(n)$, they are interpolated and recombined using the synthesis filter bank $G_i(z)$ to form a fullband cancelling noise $y'(n)$, which is used to drive the secondary source. The residual noise signal $e(n)$ is obtained by acoustically superimposing the filtered cancelling noise $y''(n)$ with the primary noise $d(n)$ through an error microphone. The SBANE decomposes the residual noise signal into subband residual noises $e_i(n)$ via the same analysis filter bank $H_i(z)$. These subband residual noises are fed back into their respective subband adaptive filters.

The number of tap-weights K for each subband adaptive filter can be determined by the ratio of the number of tap-weights M for the fullband adaptive filter to the decimation rate D , i.e., $K = M / D$. Also, due to the decimation rate D , tap-weights of all the subband adaptive filters are updated only once in every D samples. The weight-update equation for the i th subband adaptive filter is

$$\mathbf{w}_i(n+1) = \mathbf{w}_i(n) + \mu \mathbf{x}'_i(n) e'_i(n), \quad (10)$$

where the subband tap-weight vector for the i th subband is

$$\mathbf{w}_i(n) = [w_{i_0}(n) \quad w_{i_1}(n) \quad \cdots \quad w_{i_{K-1}}(n)]^T, \quad (11)$$

the subband filtered reference noise vector is

$$\mathbf{x}'_i(n) = \hat{s}_i(n) * \mathbf{x}'(n), \quad (12)$$

and the subband pseudo error is

$$e'_i(n) = e_i(n) - \hat{s}_i(n) * c_i(n) * y_i(n). \quad (13)$$

In (13), $\hat{s}_i(n)$ is the impulse response of subband secondary path estimate, $c_i(n)$ is the subband shaping filter, and $y_i(n)$ is

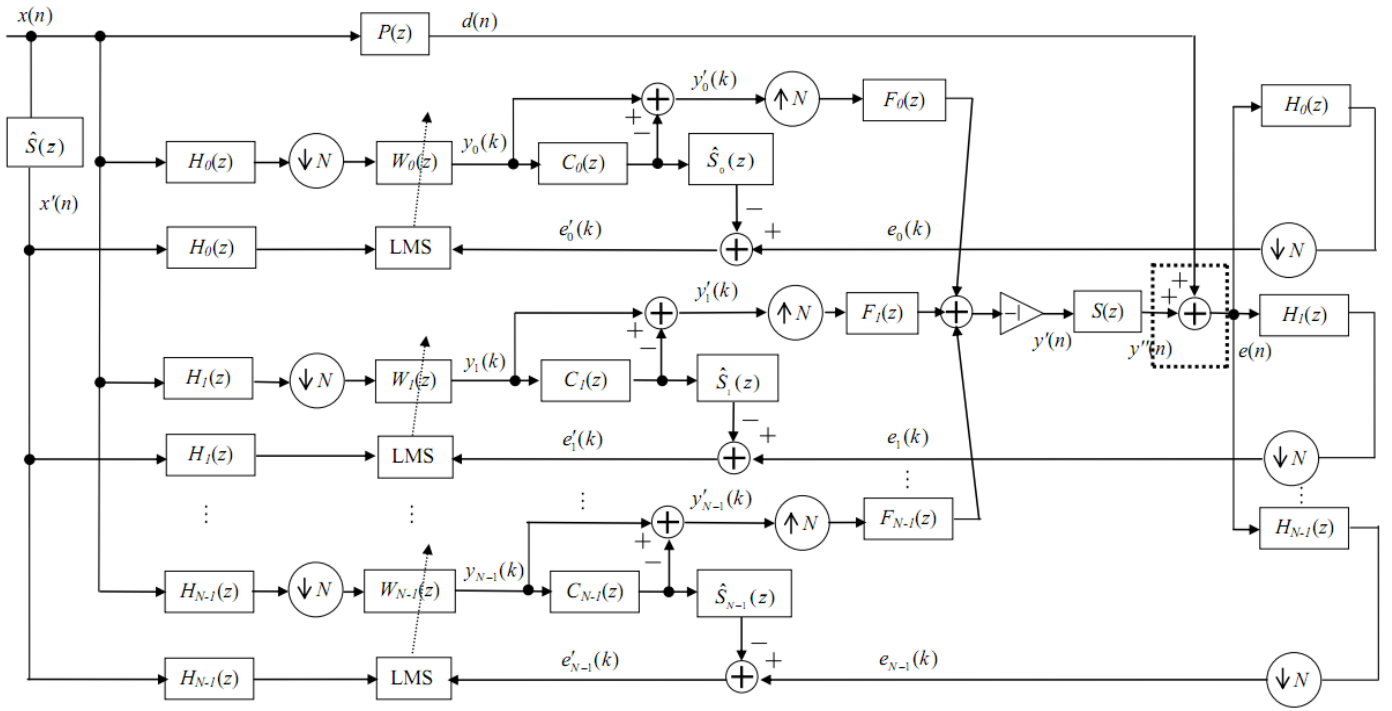


Fig. 3 Block diagram of proposed subband-based ANE for motorcycle helmet

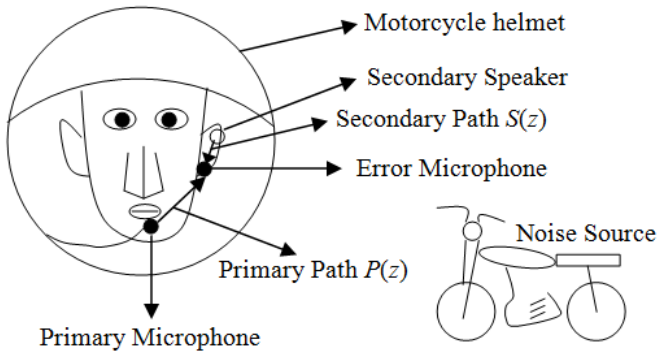


Fig. 4 Primary and secondary paths in realistic helmet ANE environment

the output of subband adaptive filter.

Here, the step-sizes for different subbands are assumed to be the same for convenience, but they can be different (usually normalized) to respond to different adaptive strategies. Since step-size is directly related to the convergence rate of each subband adaptive filter, subbands with greater noise power have smaller upper step-size bounds as compared to subbands with lower noise power.

The design of the filter bank can be accomplished by designing a pseudo-quadrature mirror filter (PQMF) bank, which has already been commonly used in MPEG-1 and MPEG-2 audio coding [3] for performing time-to-frequency mapping. As indicated by its name, a PQMF bank does not achieve perfect reconstruction, whereas in general, it has a near-perfect reconstruction. For PQMF bank design, a low-pass prototype filter $q(n)$ is first designed, and the rest of $N-1$

filters are derived simply by modulating the prototype filter with cosine terms $\cos[\pi/N(i+0.5)(n-(L-1)/2)+\theta_i]$ for $i = 0, 1, \dots, N-1$, where $\theta_i = (-1)^i \pi/4$ and L is the length of the prototype filter $q(n)$. For the synthesis filters, they are just time-reversed versions of the analysis filters. To summarize, the analysis filter $H_i(z)$ and the corresponding synthesis filter $G_i(z)$ can be represented as follows:

$$\begin{aligned} h_i(n) &= 2q(n) \cos\left[\frac{\pi}{N}(i+0.5)\left(n-\frac{L-1}{2}\right)+\theta_i\right], \\ g_i(n) &= 2q(n) \cos\left[\frac{\pi}{N}(i+0.5)\left(n-\frac{L-1}{2}\right)-\theta_i\right], \end{aligned} \quad (14)$$

where $h_i(n)$ is the impulse response of $H_i(z)$ and $g_i(n)$ is the impulse response of $G_i(z)$.

SBANE decomposes the broadband signal into several subbands, which can coincide with the critical bandwidth of human hearing. Therefore, SBANE can be spectrally shaped based on psychoacoustics findings. According to the ISO 226: 2003 normal equal-loudness-level contours [5], human hearing is not equal for all frequency components of audible sound. The equal-loudness contours show the subjective frequency response of the human ear at different sound pressure levels. In general, with the same sound pressure level, human ear is less sensitive to noise in the low-frequency region < 1000 Hz, and high frequency region > 8000 Hz. In order to compensate for this effect, five subband shaping filters $C_i(z)$ are designed to match the equal-loudness contours, so that the residual noise has a similar spectrum shape as the equal-loudness contours.

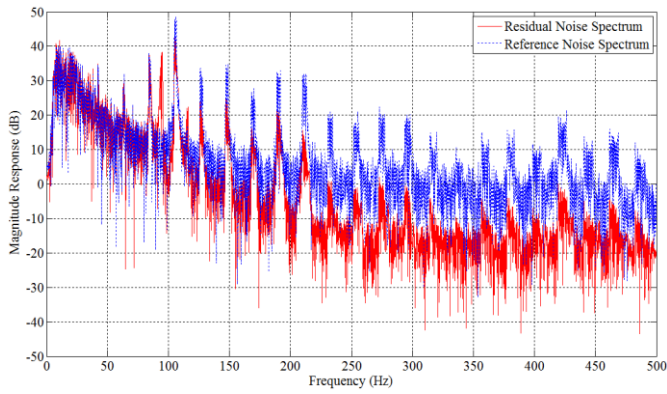


Fig. 5 Comparison of reference noise spectrum and residual noise spectrum

In order to achieve this compensation, the lower frequency components of the residual noise may need to be enhanced, whereas the higher frequency components should be attenuated. Hence, the gains of the five subband shaping filters can be designed to be 15 dB, -10 dB, -30 dB, -30 dB and -30 dB.

IV. SIMULATION RESULTS

Computer simulation is conducted to evaluate the performance of the proposed subband-based ANE. In order to obtain real motorcycle noise, a motorcycle model of Harley Davidson's Heritage Softtail with a two-cylinder, 4-stroke engine was used. The motorcycle noise was recorded using the 722 high-resolution digital audio recorder.

In order to measure the transfer functions of both the primary path and secondary path for conducting the computer simulation, an experimental setup shown in Fig. 4 was built. The system consists of one primary microphone, one error microphone and one secondary speaker. The primary speaker is placed 65 cm away from the rider (emulated by a B&K torso and head simulator, KEMAR). A motorcycle helmet is put on the head of a "dummy rider" (or KEMAR) and the secondary speaker is installed inside the helmet. The error microphone is placed near one of the ear of the KEMAR, and the primary microphone is placed near the mouth of the KEMAR to function as a communicating microphone.

For demonstration purpose, the first subband shaping filter $C_0(z)$ is designed to be an all-pass filter with a gain of 0 dB so that the frequency components from 0 to 100 Hz of the motorcycle noise will be passed without any cancellation. The second subband shaping filter $C_1(z)$ is designed with a flat gain of -10 dB so that the frequency components from 100 to 200 Hz of the motorcycle noise will be attenuated by 10 dB. The last three subband shaping filters $C_2(z)$, $C_3(z)$ and $C_4(z)$ are designed to be all-pass filters with a gain of -20 dB so that the frequency components from 200 to 500 Hz of the motorcycle noise are attenuated by 20 dB.

The recorded motorcycle noise is decimated to 1 kHz before being processed by the SBANE. Since the five-band

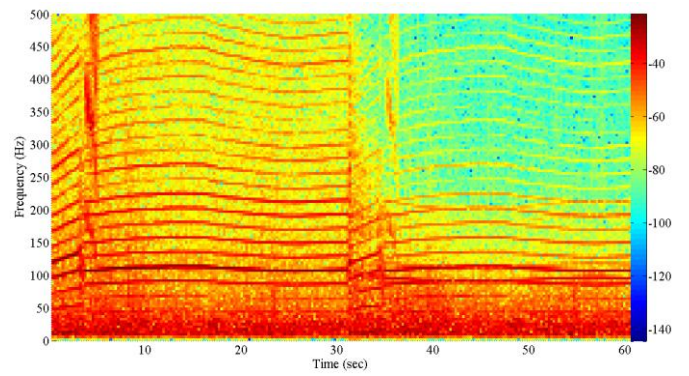


Fig. 6 Spectrogram of error signal showing the transition from subband-based ANE OFF to subband-based ANE ON

SBANE is critically sampled, each subband only operates at 200 Hz. The length of the analysis filters $H_i(z)$ and the synthesis filters $G_i(z)$ is 80 for $i = 0, 1, \dots, N-1$, and all five subband adaptive filters have length of 160. Both the primary and secondary paths are modeled using 400-tap FIR filters.

The spectrum of the reference noise and residual noise are shown in Fig. 5, which shows that the frequency components from 0 to 100 Hz of the residual noise are almost unaffected, whereas the frequency components from 100 to 200 Hz are attenuated by around 10 dB and those from 200 to 500 Hz are attenuated by around 20 dB. This confirms the shaping capability of the proposed subband-based ANE.

The shaping capability of the proposed subband-based ANE can also be observed from the spectrogram of error signal when the subband-based ANE is turned on after 30 seconds as shown in Fig. 6. Based on the previous shaping filter characteristics, a gradual increased in attenuation of noise signal at higher frequency can be easily observed.

The convergence rate of the proposed subband-based ANE and conventional ANE is also compared in terms of the mean-square error (MSE), which is shown in Fig. 7. It is found that the proposed subband-based ANE converged around 10000 samples, but the fullband ANE only converged after 15000 samples. Hence, we can conclude that the proposed subband-based ANE converges faster than the fullband ANE. The reason for this faster convergence is due to the smaller spectral dynamic range (or smaller eigenvalue spread) for each subband signal as compared to the fullband signal.

We can also take into account of the equal-loudness compensation in the human hearing mechanism to determine the amount of gain in each subband so that equal-loudness can be achieved to control engine noise. In other words, we want all the noise level in each critical band to sound almost equal, and achieve uniform noise attenuation perceptually. Hence, the gains of the five subband shaping filters are designed to be 15 dB, -10 dB, -30 dB, -30 dB and -30 dB, so that the spectrum of the residual noise has a similar shape as the equal-loudness contours, which can be easily observed from Fig. 8.

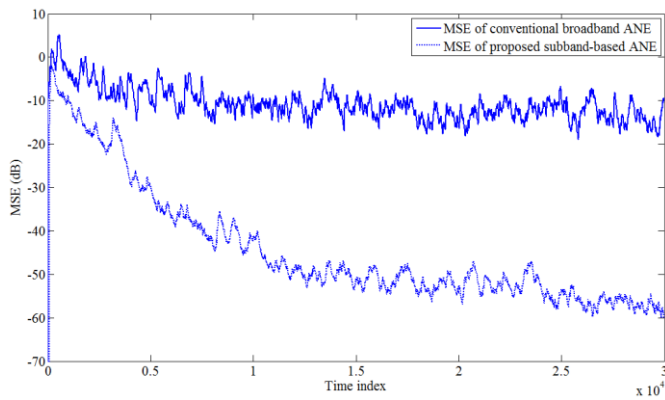


Fig. 7 Comparison of MSE for proposed subband-based ANE and fullband ANE

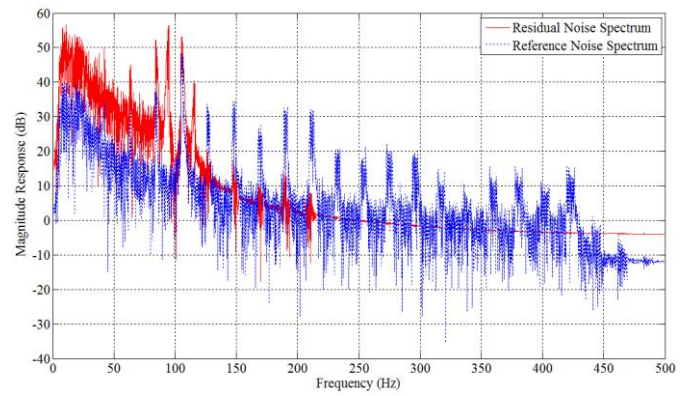


Fig. 8 Comparison of reference noise spectrum and residual noise spectrum considering equal-loudness compensation

V. CONCLUSIONS

This paper presented the subband-based active noise equalizer (SBANE) for motorcycle helmets to effectively and efficiently shape the spectrum of the residual noise as desired. The performance of the proposed system was evaluated with the computer simulations using recorded motorcycle noise and measured transfer functions of primary and secondary paths from the experimental setup. Psychoacoustics treatment can also be easily incorporated using the proposed subband-based ANE. The equal-loudness compensation can be used to control the spectrum shape of the residual noise. Simulation results show that different levels of noise control can be applied to the noise component over the critical bandwidth of the human hearing in order to retain different engine noise signature and achieve good noise reduction at the same time.

REFERENCES

- [1] K.P. Raghunathan, S.M. Kuo, and W.S. Gan, "Active Noise Control for Motorcycle Helmets," in *Proc. 2010 International Conference on Green Circuits and Systems*, June 2010, Shanghai, China (Invited Paper).
- [2] S.M. Kuo and Y. Yang, Broadband Adaptive Noise Equalizer, *IEEE Signal Processing Letters*, 3 (1996) pp. 234-235.
- [3] K.A. Lee, W.S. Gan, and S.M. Kuo, *Subband Adaptive Filtering: Theory and Implementation*, John Wiley, 2009.
- [4] S.M. Kuo, R.K. Yenduri, and A Gupta, "Frequency-Domain Delayless Active Sound Quality Control Algorithm," *Journal of Sound and Vibration*, 318 (2008), pp. 715-724.
- [5] BS ISO, 226: British Standard Specification for Normal Equal-Loudness-Level Contours for Pure Tones under Free-Field Listening Conditions, 2003.
- [6] ANSI S1.4: Specifications for Integrating-averaging Sound Level Meters, 1983.
- [7] ANSI S1.42: American National Standard Design Response of Weighting Networks for Acoustical Measurements, 2001.